Constrained Model Predictive Control Implementation for a Heavy-Duty Gas Turbine Power Plant

HADI GHORBANI*
Msc. Student of Mechanical Engineering
ghorbani.hadi@gmail.com

ALI GHAFFARI**
Prof. of Mechanical Engineering
ghaffari@kntu.ac.ir

MEHDI RAHNAMA***
Msc. Student of Electrical Engineering
mehdi.rahnama@gmail.com

* ,** Department of Mechanical Engineering
K.N.Toosi University Of Technology,
Pardis Avenue, Mollasadra Street, Tehran,
IRAN

*** Islamic Azad University of Science & Research branch, Tehran Iran
Deputy of Operation Department of Montazer Ghaem CCPP

Abstract: In this paper, model predictive control (MPC) strategy is implemented to a GE9001E gas turbine power plant. A linear model is developed for the gas turbine using conventional mathematical models and ARX identification procedure. Also a process control model is identified for system outputs prediction. The controller is designed in order to adjust the exhaust gas temperature and the rotor speed by compressor inlet guide vane (IGV) position and fuel signals. The proposed system is simulated under load demand disturbances. It is shown that MPC controller can maintain the rotor speed and exhaust gas temperature more accurately in comprehension with both SpeedTronic™ control system and conventional PID control.

Key-words: Gas turbine, Identification, ARX, Predictive control, Power plant, Modeling, Multivariable control, PID

1. Introduction

Recently, gas turbines have found increasing service in the world because of their compactness, multiple fuel applications, fast start-stop sequence and etc. So the use of gas turbines has quickly become greater in power supply industry following the deregulation of electricity.
As a brief survey in the history of gas turbine studies, a simplified mathematical model consist of a set of algebraic equations and related temperature, speed and acceleration controllers is provided by W.I.Rowen in 1983 [1]. Then it is modified by adding the influence of variable inlet guide vanes (VIGV) [2] and this frequency-domain model is validated by L.N.Hannet [3]. Physically based model to determine frequency dependency and a neural network simulator are other gas turbine models ([4], [5]). The identification techniques have been concerned mainly about aircraft gas turbine engines [6]. A low order linear model using Box-Jenkins algorithm of a micro-turbine is presented by Jurado and Cano [7].
MPC is a control strategy which has developed considerably nowadays in a wide variety of application areas including power plants, chemical industries and etc. The main reason for this is that it is the only generic control technology which can deal routinely with equipments and safety constraints. Also it is more powerful than PID control, even for single loops without constraints, without being much more difficult to tune, even on difficult loops such as those containing long time delays [8]. Model predictive control strategy uses a model of system to predict the response over a future interval called predicting horizon [9]. The various MPC algorithms only differ among themselves in the model used to represent the process and the noise where cost function is minimized [10].
The application of Model Predictive Control (MPC) to control gas turbine is introduced by Vroemen and Essen

in ([12],[13]). Junxia presents an approximate model predictive control used to control shaft speed of a gas turbine engine in [14]. Moreover, a model based predictive control is applied on the gas turbine plant using Hammerstein model and GPC algorithm [15].
In this paper MPC controller is investigated for a MS9001E gas turbine (mounted in Montazer Ghaem power plant) in order to control speed and exhaust gas temperature by considering I/O constraints and using GPC algorithm. The plant model is identified using Rowen conventional model and ARX techniques. Also a model is identified as process model in order to predict future outputs. Disturbances and measurement noises are considered and a state observer is designed for estimating states which are not possible to measure them. Finally system is simulated under a step load demand disturbance and MPC is compared with conventional PID control. Then both MPC and PID controllers are evaluated by the SpeedTronic™ control system using load increasing field data.

2. Gas Turbine System Description

According to the Brayton cycle, an ideal gas turbine system consists of both isentropic and isobar processes thermodynamically. Thus heavy-duty gas turbine includes combustion chambers, a multi stages axial flow compressor connected to a multi stages expansion turbine which drives an electric generator for electrical power supply. The inlet air flow rate is maintained by guide vanes (VIGV) in the compressor entrance.
Temperature of the gases entering the turbine cannot exceed the limit imposed by the high temperature resistance of the materials. Nevertheless, if this temperature decreases too much, the plant (both gas turbine and HRSG) efficiency would become unacceptably low. Therefore, turbine firing temperature (T_f) must be kept under a higher limit (technical) and over a lower limit (economical), as close as possible to the optimum point [11]. According to the thermodynamic explanations, the firing temperature is presented by the following relation [3];

$$T_f(W_a, W_f, T_a, X) = T_D \frac{W_f}{W_a}.K + T_a\left[1 + \frac{(X-1)}{\eta_{comp}}\right] \qquad (1)$$

Here X is defined as $[CPR \times W_a]^{\frac{\gamma-1}{\gamma}}$
In the SpeedTronic™ Mark IV, quantities T_f and air flow rate (w_a) are not measured directly because of some technical considerations. Therefore, T_f is maintained by means of exhaust gas temperature (T_x) and compressor discharge pressure (CPD) in practice where T_x can be expressed by relation the following relation [2];

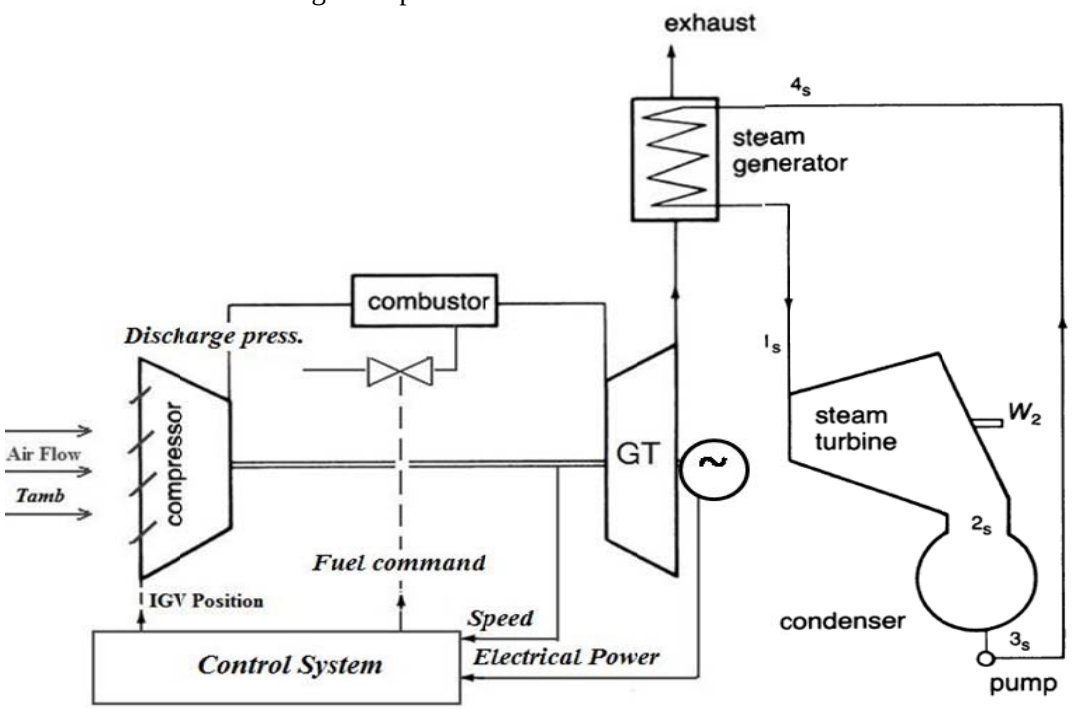

Figure 1- Gas turbine system overview

$$T_x(T_f, X, \eta_{Turbine}) = \left[1-(1-\frac{1}{X})\eta_{Turbine}\right]T_f \quad (2)$$

Parameters T_x and CPD are system main outputs which explain combustion quality indirectly and are correspondent to the T_f and W_a respectively. Parameters W_a and CPD, vary with ambient air temperature T_{amb}, shaft speed ω and IGV variations by considering constant site pressure. Also exhaust gas flow rate W_x can be assumed equal to the W_a eliminating fuel flow rate (W_f) against the W_a in the combustor (see [2],[4]). Consequently, G and F are nonlinear functions which express CPD and T_x respectively by means of independent variables by the following relations;

$$CPD = G(T_{amb}, IGV, \omega) \quad (3)$$

$$T_x = F(T_{amb}, IGV, \omega, W_f) \quad (4)$$

Turbine output torque is not appreciably affected by guide vane action and can be estimated to within 0.05 per unit accuracy ([2],[3]) by following relation;

$$T_{out} = \frac{1.16\,(W_f - 1.33)}{\omega} \quad (5)$$

Instead using fuel flow command and mechanical power, it is possible to relate them with FSR (fuel stroke reference) signal and electrical power output respectively (see [2],[4]). By using fuel command, the dynamics of stop-ratio and control valves are taken into account with combustion system. In addition, the electrical generator and rotor dynamics are considered altogether in the power system. Figure 1 illustrates the gas turbine cycle overview schematically.

3. Gas Turbine Plant Identification

In order to describe gas turbine system as close as possible to the real system, it is necessary to identify its behavior based on I/O related signals. Exploiting Rowen conventional models ([1],[2]), a nonlinear block diagram model is obtained which is illustrated in Figure 2.

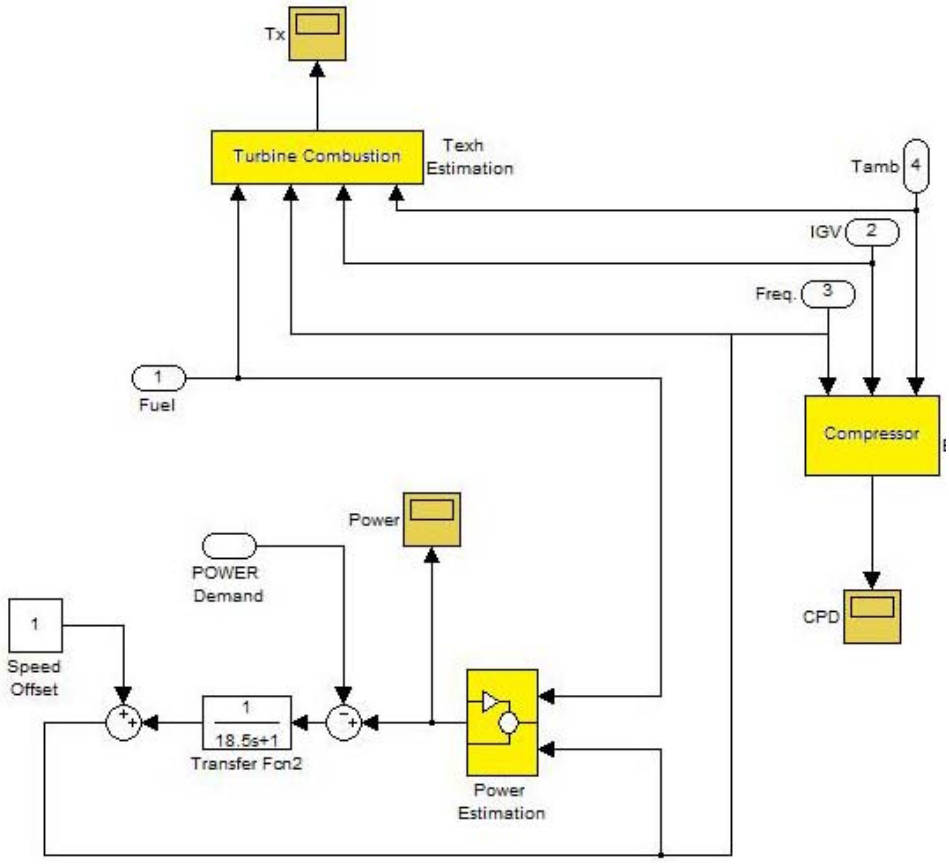

Figure 2- Gas Turbine plant model block diagram
(Each block transfer functions are presented in Appendix A)

In this mathematical model, the exhaust gas temperature, compressor pressure discharge and output electrical power quantities are estimated using the second order ARX identification techniques [16].

The loss function, FEP and fitness percent are determined in order to evaluate model. FPE is defined as *Akaike's forward Prediction Error* by equation 6:

$$FPE = V \times \frac{1 + d/N}{1 - d/N} \qquad (6)$$

Where *d* is the number of estimated parameters and *N* is number of estimation data. The loss function $V_N(\theta, Z^N)$ is defined as normalized sum of squared prediction errors.

$$V_N(\theta|Z^N) = \frac{1}{N}\sum_{t=1}^{N}\{y(t) - \hat{y}(t|\theta)\}^2 \qquad (7)$$

In order to fit models by regressors to data set, it is pointed out the PEM (prediction-error identification method) procedure using a *LSM* algorithm. Validation the obtained model is done by *Residual* (prediction error) analysis tests which consist of *whiteness test* and *independence test*.

4. MPC controller design

According to the predictive controller strategy, future outputs are predicted at each time instant for a determined prediction horizon H_p by using a process model. These predicted outputs at time $(t+k)$, $y(t+k|t)\ for\ k = 1, \dots, H_p$, depend on both past I/O data and future control signals $u(t+k|t), k = 0, \dots, H_p - 1$. The future control signals are calculated by optimizing a determined criterion to keep the process as close as possible to the reference trajectory $w(t+k)$. This criterion takes the form of the quadratic function of the errors between the predicted output signal and predicted reference.

The control strategy in this paper is keeping the shaft speed constant when the power demand rises. The manipulated control signals are fuel command (FSR) and the IGV position command considering the constraints on fuel and actuators. The exhaust gas temperature cannot exceed its allowed range during this process. Also the power demand and ambient air temperature variations are system measurable disturbances.

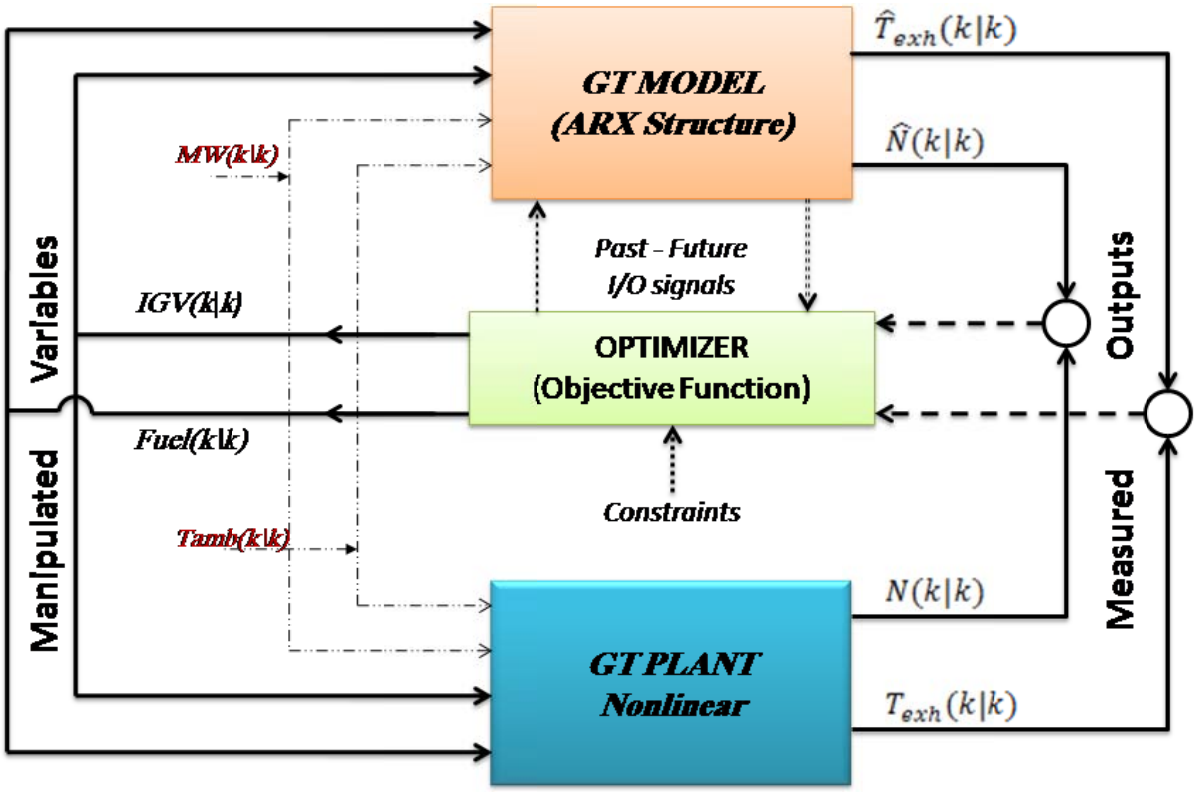

Figure 3- MPC strategy used for gas turbine control

The MPC algorithm computes the control sequence minimizing following quadratic cost function.

$$J(H_{p1}, H_{p2}, H_c, \lambda) = \sum_{J=H_{p2}}^{H_{p2}} \left(w(k+j) - \hat{y}(k+j)\right)^2 + \lambda \sum_{j=0}^{H_c} \Delta u^2(k+j-1) \qquad (8)$$

Here H_{p1} *and* H_{p2} are minimum and maximum predicting horizons respectively. The H_c is the control horizon and λ is the move suppression coefficient. The strategy used to control gas turbine system is presented in Figure 3.

A gas turbine control model (process model) is used to predict system future parameters. The model which is exploited in this paper is a linear time invariant system described by the following equations.

$$\begin{aligned} x(k+1) &= Ax(k) + B_u u(k) + B_v v(k) + B_d d(k) \\ y_m(k) &= C_m x(k) + D_{vm} v(k) + D_{dm} d(k) \\ y_u(k) &= C_u x(k) + D_{vu} v(k) + D_{du} d(k) + D_{uu} u(k) \end{aligned} \qquad (9)$$

Where;

$x(k)$: $n_x$dimensional model states vector

$u(k)$: n_u dimensional manipulated variables vector

$v(k)$: n_v dimensional measured disturbances vector

$d(k)$: n_d dimensional unmeasured disturbances

$y_m(k)$: measured outputs

$y_u(k)$: unmeasured outputs

This process model is identified exploiting ARX identification method. The related loss function and FPE are calculated 0.000313534 and 0.000337166 respectively. Noting that all state variables of the plant are not measurable, a state observer is designed in order to estimate inaccessible states.

The measurements update equation is given by,

$$\begin{bmatrix} \hat{x}(k|k) \\ \hat{x}_d(k|k) \\ \hat{x}_m(k|k) \end{bmatrix} = \begin{bmatrix} \hat{x}(k|k-1) \\ \hat{x}_d(k|k-1) \\ \hat{x}_m(k|k-1) \end{bmatrix} + M\left(y_m(k) - \hat{y}_m(k)\right) \qquad (10)$$

and the time update equation is:

$$\begin{bmatrix} \hat{x}(k+1|k) \\ \hat{x}_d(k+1|k) \\ \hat{x}_m(k+1|k) \end{bmatrix} = \begin{bmatrix} A\hat{x}(k|k) + B_u u(k) + B_v v(k) + B_d \bar{C}\hat{x}(k|k) \\ \bar{A}\hat{x}_d(k|k) \\ \tilde{A}\hat{x}_m(k|k) \end{bmatrix} \qquad (11)$$

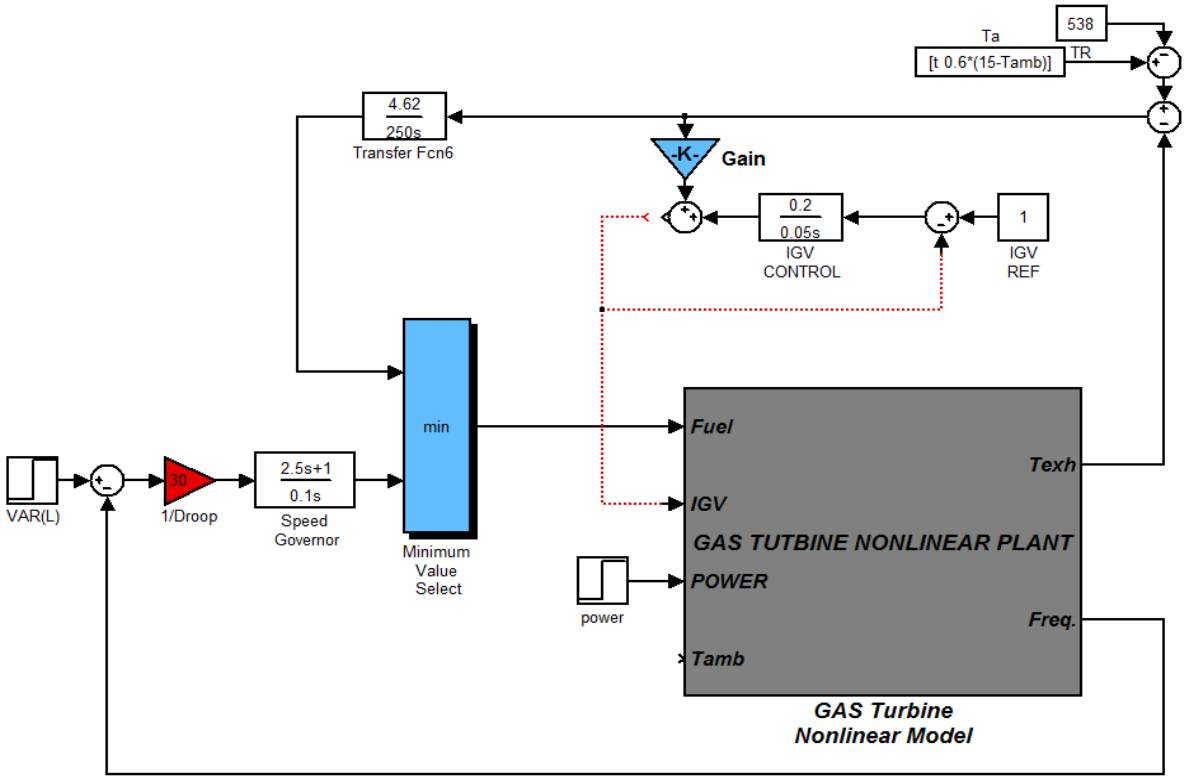

Figure 4-Block diagram gas turbine classic control model [2]

Finally the correction equation is:

$$\hat{y}_m = C_m\hat{x}(k|k-1) + D_{vm}v(k) + D_{dm}\bar{C}\hat{x}_d(k|k-1) + \tilde{C}\hat{x}_m(k|k-1) \quad (12)$$

Here gain M is applied to minimize the estimation error covariance in the Kalman filter because of measurement noises. Also x_d and x_m are disturbance and measurement noise states. The control model parameters are presented in Appendix B.

The constraints which are applied to this controller are expressed by the following equations:

$$u_{min} \le u(k+j) \le u_{max} \; for \; j = 1, \dots, H_c$$
$$y_{min} \le y(k+j) \le y_{max} \; for \; j = 1, \dots, H_p \quad (13)$$

5. Results and Discussion

5.1 Plant model identification

Data sampling is collected for full speed, no load, to full load conditions (81.6 MW base load) with sampling interval equal to 1.0 sec. During collecting data, the HRSG is started and consequently the related steam turbine is paralleled to the network. Due to the starting HRSG and gas turbine loading, the control module is on manual mode. Therefore, operator controls the guide vane manually. The site ambient temperature variations are measured about 28 to 32 $^{\circ}C$.

Recorded input signals are air temperature (T_{amb}), shaft speed (ω), IGV position (θ_{IGV}) and FSR where the exhaust gas temperature (T_x), compressor pressure discharge (*CPD*) and electrical power (*Pe*) are output signals. The identified model specifications are illustrated in Table 1 and model validation analysis test results are given in Figure 5.

Table 1- ARX identified plant model characteristics

	Loss Function	FPE	Fit%
T_x	22.25	25.33	93.36
CPD	0.0005085	0.0005641	95.43
P_e	0.0000828	0.00008951	92.82

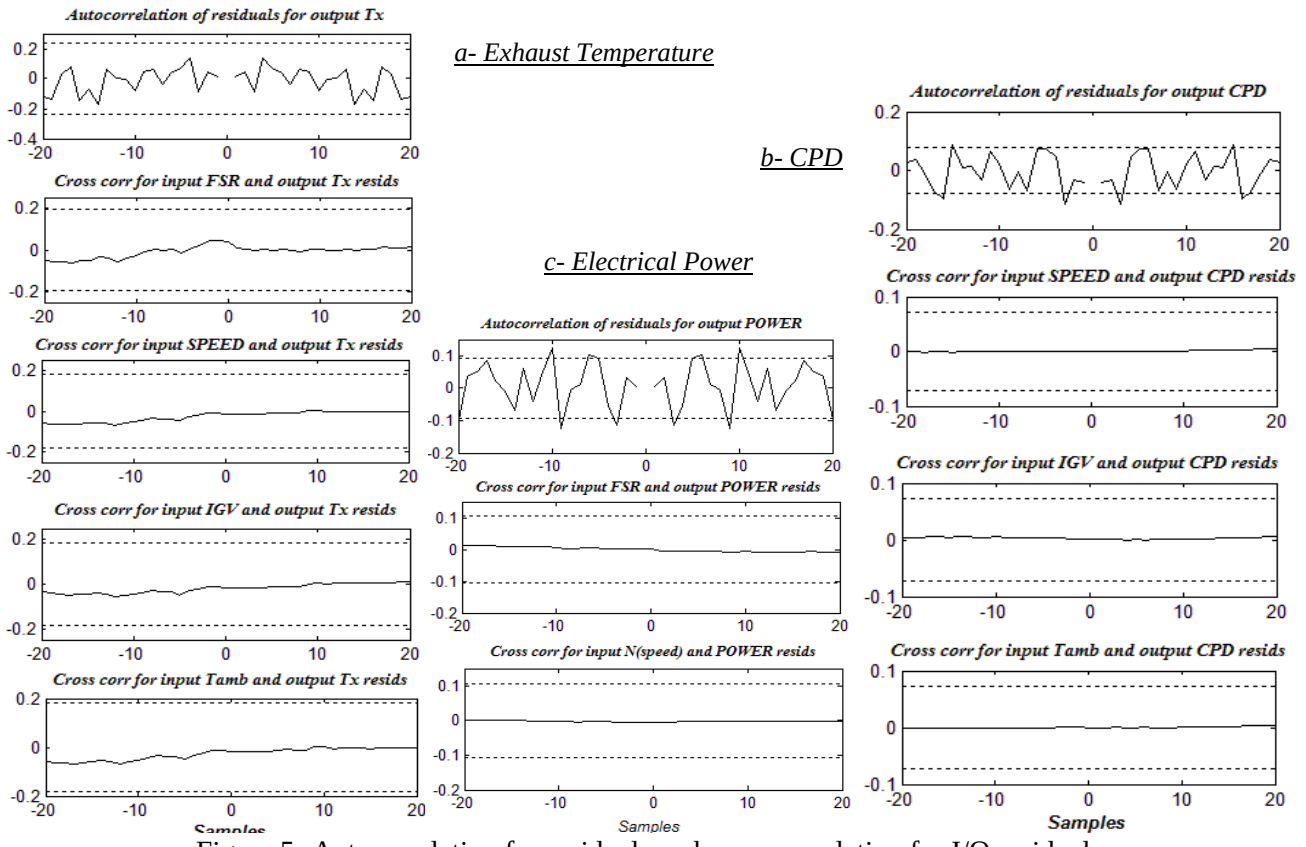

Figure 5- Autocorrelation for residuals and cross correlation for I/O residuals

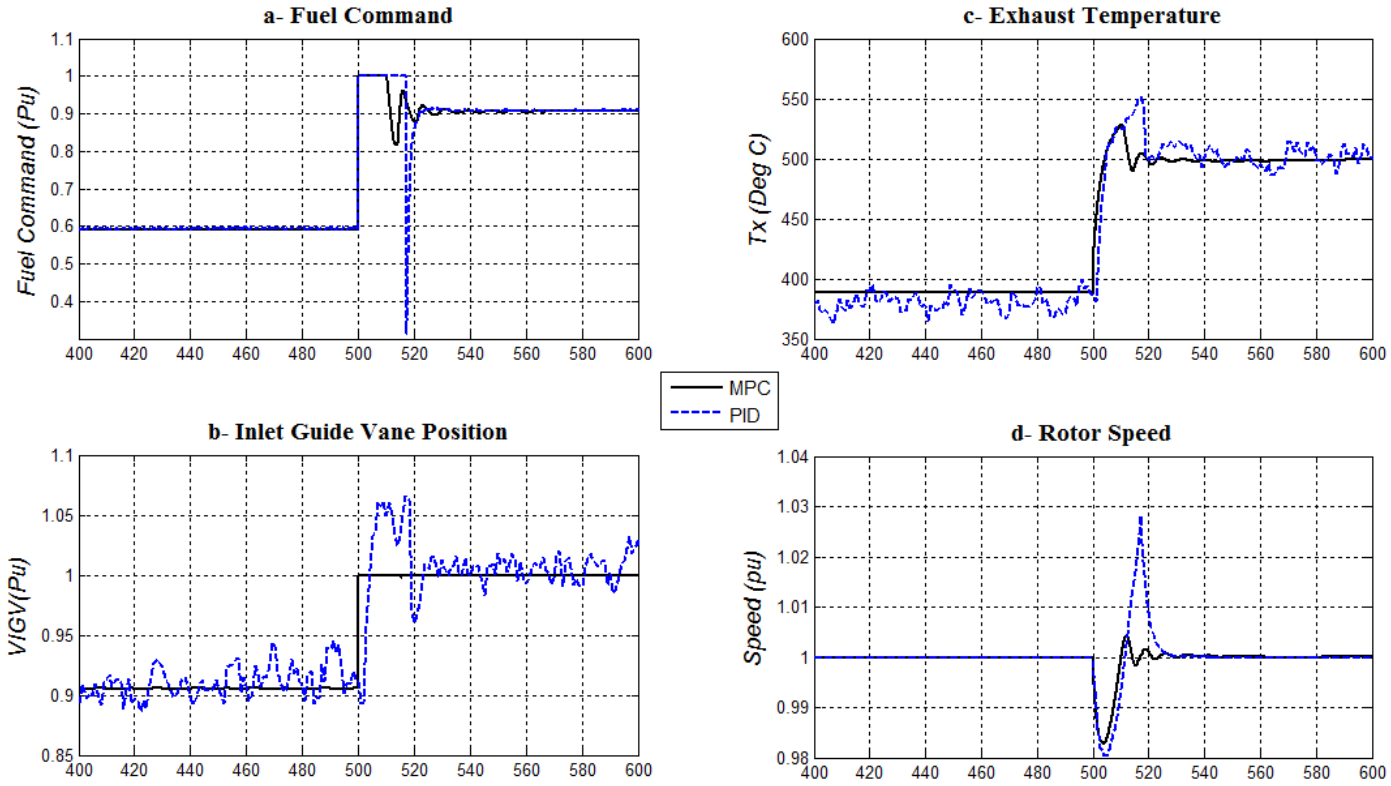

Figure 6- Step Response Under 0.4 per unit Load increasing

5.2 Controller parameters

Considering the actuators working range and flame stability, the input constraints are applied as $\begin{bmatrix}0.1935\\0.67\end{bmatrix} \leq \begin{bmatrix}\text{FSR}\\\text{IGV}\end{bmatrix} \leq \begin{bmatrix}1\\1\end{bmatrix}$. The high variations of the turbine speed can cause defects on network frequency and exhaust temperature, T_x, must be limited because of economical and physical considerations. So output constraints are taken into account as $\begin{bmatrix}0.995\\270\end{bmatrix} \leq \begin{bmatrix}N\\Tx\end{bmatrix} \leq \begin{bmatrix}1.005\\536\end{bmatrix}$.

In order to avoid the calculation time, control horizon H_c must be no longer than the output lag terms. Consequently, H_c is set equal to 1 sampling period.

Since H_{p1} is usually equal to the model delay time, it is taken equal to zero. The H_{p2} must be taken close to the rise time of the system. Nevertheless, choosing it too long requires much more calculation time. Considering the sample time equal to 0.01 sec, it is shown that the best performance is obtained letting H_{p2} equal to 0.03 sec (3 sampling period).

Manipulated control inputs are weighted as 0.1 and 0.12 for FSR and IGV respectively and their rising rate weights are chosen 0.1.

The conventional PID control shown in Figure 4 [2]used to compare with the proposed MPC system. The related fuel command signal is a minimum value between speed and temperature control loop commands. The IGV position is manipulated in order to control the exhaust gas temperature when the steam turbine is paralleled to the gas turbine in combined cycle.

5.3 Simulation Results

The proposed MPC control system is modeled dynamically with MATLAB SIMULINK. First an electrical power increase is applied to the model by a step value equal to 0.4 per unit. Comprehensive results between MPC and the PID classical control are presented in Figure 6. It is shown that the control aspects are well complied exploiting MPC and response overshoots and oscillations are considerably improved.

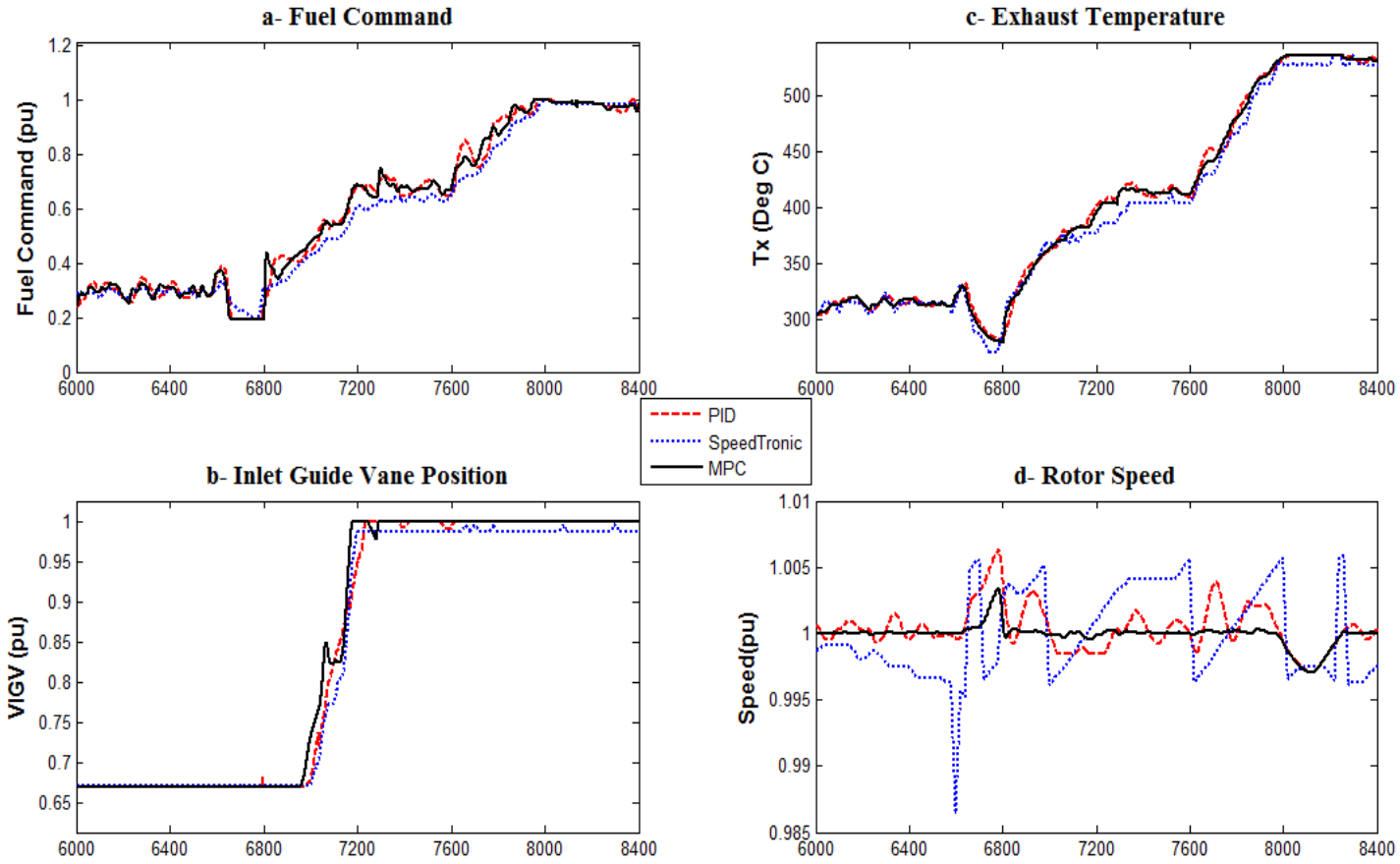

Figure 7- MPC in comprehension with both PID classical control and SPEEDTRONIC™ control system

Then the model is compared with the SpeedTronic™ control system in a real load demand conditions when the ambient air temperature is varied between 28C to 32C during 14000 seconds. The constant rotor speed and exhaust gas temperature are obtained by manipulating the FSR and IGV signals which is illustrated in Figure 7. In comprehension with the SpeedTronic™, the rotor speed is improved perfectly under these circumstances with increasing the fuel consumption (Figure 7-a, d). The reason of this increase is that IGV manipulates the gas exhaust temperature with low effect on output power and speed control using guide vane position is not possible. Therefore, constant speed is attained by fuel control and it needs much more fuel consumption in order to overcome rotor inertia. Consequently, increasing the exhaust temperature is necessary when the load demand increases (Figure 7-b, c).

6. Conclusion

In this paper, MPC controller is implemented for a MS9001E gas turbine (mounted in Montazer Ghaem power plant) in order to control speed and exhaust gas temperature. The I/O constraints are considered and a GPC algorithm is designed. The plant model is identified using Rowen conventional model and ARX techniques in order to simulate compressor pressure discharge, exhaust gas temperature and electrical power. Also a model is identified as process model in order to predict future outputs. Disturbances and measurement noises are considered and a state observer is designed for estimating inaccessible state variables. Also system is simulated under a step load demand disturbance and results are presented in comprehension with classical PID controller. Finally, a load disturbance is applied to the model based on real field data and designed controller is compared with both SpeedTronic™ and PID control systems. Results show that MPC control can give a constant speed when the system is subjected to a load demand disturbance simultaneous perfect temperature control.

7. Nomenclatures:

ARX	*Auto Regressive with eXogenous inputs*
CPD	*Compressor Pressure Discharge*
CPR	*Compressor Pressure Ratio*
FPE	*Akaike's Forward Prediction Error*
FSR	*Fuel Stroke Reference*
GPC	*Generalized Predictive Control*
H_p	*Prediction Horizon*
H_c	*Control Horizon*
IGV	*Inlet Guide Vanes*
LSM	*Least Square Method*
T_{amb}	*Ambient Air Temperature*
T_f	*Firing Temperature*
T_{out}	*Turbo Generator Torque*
T_x	*Exhaust Gas Temperature*
W_a	*Air Flow rate*
W_f	*Fuel Flow rate*
W_x	*Exhaust Gas Flow rate*
θ	*Unknown Parameters Vector*
φ	*Regression vector*
η	*Turbine Efficiency*

References:

[1] W.I.Rowen, Simplified Mathematical Representation of Heavy-Duty Gas Turbines, *ASME Journal of Engineering for Gas Turbines and Power, vol. 105,1983*

[2] W.I.Rowen , Simplified Mathematical Representation Of Single Shaft Gas Turbines in Mechanical Drive Service, *The International Congress and Exposition , 1992*

[3] L.N.Hannet, Afzal Khan, Combustion Turbine Dynamic Model Validation from Tests, *IEEE Transaction on Power System, Vol.8, No. 1, 1993*

[4] K.Kunitomi , A.Kurita , H.Okamoto and Y.Tada, Modeling Frequency Dependency Of Gas Turbine Output, *IEEE 2001*

[5] C. Boccaletti, G. Cerri, and B. Seyedan, Neural Network Simulator of a Gas Turbine With a Waste Heat Recovery Section, *ASME Journal of Gas Turbines and Power, Vol.123, 2001*

[6] N.Chiras, C.Evans, D.Rees., Global Nonlinear Modeling of Gas Turbine Dynamics Using NARMAX Structures, *ASME Journal of Gas Turbines and Power,Vol. 124, 2002*

[7] Jurado F, Cano A, Use of ARX algorithms for modelling micro-turbines on the distribution feeder, *IEE Proc Generat Transm Distribut 2004*

[8] J.M.Maciejowski, *Predictive Control with Constraints*, Prentice Hall 2002

[9] S. Joe Qin , Thomas A. Badgwell, A survey of industrial model predictive control technology, *PERGAMON Journal of Control Engineering Practice 11 (2003)*

[10] E.F.Camacho, C.Bordons, *Model Predictive Control* , 2nd Edition, Springer 2004

[11] Working Group on Prime Mover and Energy Supply Models for System Dynamic Performance Studies, 'Dynamic Models for Combined Cycle Plants in Power System Studies, *IEEE Transaction on Power Systems, Vol. 9, No. 3, 1994*

[12] Vroemen BG, van Essen HA, van Steenhoven AA, Kok JJ., Nonlinear model predictive control of a laboratory gas turbine installation, *ASME Journal of Engineering for Gas Turbines and Power 1999*

[13] Van Essen HA, de Lange HC. Nonlinear model predictive control experiments on a laboratory gas turbine installation, *ASME Journal of Engineering for Gas Turbines and Power 2001*

[14] Junxia Mu and David Rees, Approximate Model Predictive Control for Gas Turbine Engines, *Proceeding of the 2004 American Control Conference*

[15] F. Jurado a, J. Carpio, Improving distribution system stability by predictive control of gas turbines , *Journal of Energy Conversion and Management 47 (2006)*

[16] Ljung, *L. System Identification: Theory for the User*, Upper Saddle River, NJ, Prentice-Hall PTR,

Appendix A

The plant model transfer functions for Figure 2 are presented as following based on Table 2 given I/O signals:

Table 2- I/O parameters for plant model identification

Y(t)	**U(t)** $= [u_1(t) \cdots u_m(t)]^T$
T_x	$[FSR \quad \omega \quad \theta_{IGV} \quad T_{amb} \quad 1]^T$
CPD	$[\omega \quad \theta_{IGV} \quad T_{amb} \quad 1]^T$
Pe	$[FSR \quad \omega]^T$

Turbine combustion system dynamics:

$$\frac{T_x(s)}{FSR(s)} = \frac{79.19s^2 + 344.5s + 372.3}{s^2 + 3.266s + 0.9384}$$

$$\frac{T_x(s)}{\omega(s)} = \frac{21.98s^2 + 207.6s + 327.2}{s^2 + 3.266s + 0.9384}$$

$$\frac{T_x(s)}{IGV(s)} = \frac{-119s^2 + 312.3s - 148.6}{s^2 + 3.266s + 0.9384}$$

$$\frac{T_x(s)}{T_{amb}(s)} = \frac{0.7975s^2 + 0.8849s - 1.42}{s^2 + 3.266s + 0.9384}$$

Output power estimation system:

$$\frac{P_e(s)}{FSR(s)} = \frac{0.3827s^2 + 0.8935s + 0.2562}{s^2 + 1.3331s + 0.2015}$$

$$\frac{P_e(s)}{\omega(s)} = \frac{-0.212s^2 - 0.4496s - 0.05068}{s^2 + 1.3331s + 0.2015}$$

Compressor system dynamics:

$$\frac{CPD(s)}{\omega(s)} = \frac{2.081s^2 + 5.078s + 1.833}{s^2 + 4.574s + 1.083}$$

$$\frac{CPD(s)}{IGV(s)} = \frac{-0.4447s^2 - 0.4645s + 0.8496}{s^2 + 4.574s + 1.083}$$

$$\frac{CPD(s)}{T_s(s)} = \frac{-0.06243s^2 + 0.1525s + 0.05521}{s^2 + 4.574s + 1.083}$$

Appendix B

The process model can be described by a simplified denotation as below:

$$x(k+1) = Ax(k) + Bu(k) \qquad y(k) = Cx(k) + Du(k)$$

Where A,B,C and D coefficients are given as following

$$\boldsymbol{Ax(k)} = \begin{bmatrix} 0.6897 & 7.421e-6 & 0.2019 & 1.386e-5 & 0.1036 & -1.406e-5 & -0.006072 & 0.007168 & -0.002625 & 4.694e-5 \\ -57.13 & 0.5061 & 161.1 & 0.1742 & -8.422 & 0.03467 & 70.6 & -214.2 & 86.35 & -0.4043 \\ 1 & 0 & 0 & 0 & 0 & 0 & 0 & 0 & 0 & 0 \\ 0 & 1 & 0 & 0 & 0 & 0 & 0 & 0 & 0 & 0 \\ 0 & 0 & 1 & 0 & 0 & 0 & 0 & 0 & 0 & 0 \\ 0 & 0 & 0 & 1 & 0 & 0 & 0 & 0 & 0 & 0 \\ 0 & 0 & 0 & 0 & 0 & 0 & 0 & 0 & 0 & 0 \\ 0 & 0 & 0 & 0 & 0 & 0 & 0 & 0 & 0 & 0 \\ 0 & 0 & 0 & 0 & 0 & 0 & 0 & 0 & 0 & 0 \\ 0 & 0 & 0 & 0 & 0 & 0 & 0 & 0 & 0 & 0 \end{bmatrix} \begin{bmatrix} x_1 \\ x_2 \\ x_3 \\ x_4 \\ x_5 \\ x_6 \\ x_7 \\ x_8 \\ x_9 \\ x_{10} \end{bmatrix}$$

$$\boldsymbol{Bu(k)} = \begin{bmatrix} 0.006706 & -0.01074 & 0.006172 & -3.786\text{e}-5 & 0.003951 & 0 \\ 0.003951 & 273.9 & -142.7 & 0.7871 & 0.3314 & 4.481 \\ 0 & 0 & 0 & 0 & 0 & 0 \\ 0 & 0 & 0 & 0 & 0 & 0 \\ 0 & 0 & 0 & 0 & 0 & 0 \\ 0 & 0 & 0 & 0 & 0 & 0 \\ 1 & 0 & 0 & 0 & 0 & 0 \\ 0 & 1 & 0 & 0 & 0 & 0 \\ 0 & 0 & 1 & 0 & 0 & 0 \\ 0 & 0 & 0 & 1 & 0 & 0 \end{bmatrix} \begin{bmatrix} FSR \\ MW \\ IGV \\ Tamb \\ V@N \\ V@Texh \end{bmatrix}$$

$$\boldsymbol{Cx(k)} = \begin{bmatrix} 0.6897 & 7.421e-6 & 0.2019 & 1.386e-5 & 0.1036 & -1.406e-5 & -0.006072 & 0.007168 & -0.002625 & 4.694e-5 \\ -57.13 & 0.5061 & 161.1 & 0.1742 & -8.422 & 0.03467 & 70.6 & -214.2 & 86.35 & -0.4043 \end{bmatrix} \begin{bmatrix} x_1 \\ x_2 \\ x_3 \\ x_4 \\ x_5 \\ x_6 \\ x_7 \\ x_8 \\ x_9 \\ x_{10} \end{bmatrix}$$

$$\boldsymbol{Du(k)} = \begin{bmatrix} 0.006706 & -0.01074 & 0.006172 & -3.786\text{e}-5 & 0.003951 & 0 \\ 0.003951 & 273.9 & -142.7 & 0.7871 & 0.3314 & 4.481 \end{bmatrix} \begin{bmatrix} FSR \\ MW \\ IGV \\ Tamb \\ V@N \\ V@Texh \end{bmatrix}$$